# On the mid-Pleistocene transition to 100-kyr glacial cycles and the asymmetry between glaciation and deglaciation times

Eli Tziperman and Hezi Gildor[1]

Environmental Sciences, Weizmann Institute, Rehovot, Israel

Received 30 January 2001; revised 26 June 2002; accepted 25 July 2002; published 9 January 2003.

[1] A mechanism is proposed for the mid-Pleistocene transition from a dominant periodicity of 41 kyr to 100 kyr in glacial oscillations. The same mechanism is shown to also explain the asymmetry between the long glaciation and short deglaciation phases of each cycle since that transition versus the symmetry of the 41-kyr oscillations prior to the transition. These features arise naturally within the framework of the sea-ice switch glacial cycle mechanism of *Gildor and Tziperman* [2000] as a result of the gradual cooling of the deep ocean during the Pleistocene. This cooling results in a change of the relation between atmospheric temperature and the rates of accumulation and ablation of continentals ice sheets. It is this latter change that leads to the activation of the sea-ice switch and therefore to the initiation of the 100-kyr oscillations. The gradual glaciation and rapid deglaciations during these oscillations occur because the mean value of the ice sheet ablation is not far from the maximum rate of snow accumulation during warm periods. This proximity of mean ablation and maximum accumulation rates is shown to be also a consequence of the mid-Pleistocene gradual cooling of the deep ocean. *INDEX TERMS:* 3344 Meteorology and Atmospheric Dynamics: Paleoclimatology; 1620 Global Change: Climate dynamics (3309); 1640 Global Change: Remote sensing; 4267 Oceanography: General: Paleoceanography; *KEYWORDS:* climate dynamics, glacial cycles, mid-Pleistocene transition, 100 kyr, 41 kyr

**Citation:** Tziperman, E., and H. Gildor, On the mid-Pleistocene transition to 100-kyr glacial cycles and the asymmetry between glaciation and deglaciation times, *Paleoceanography*, *18*(1), 1001, doi:10.1029/2001PA000627, 2003.

## 1. Introduction

[2] A new mechanism for the glacial-interglacial cycles has been recently introduced by *Gildor and Tziperman* [2000, 2001b] (hereafter GT). The mechanism relies on the rapid growth and melting of extensive sea-ice cover. The sea-ice cover, through its effects on the atmospheric energy balance and air-sea fluxes, is able to switch the climate system from a growing land-ice mode (glaciation) to a retreating land-ice mode (deglaciation). GT dubbed this the sea-ice switch (SIS) mechanism of glacial cycles. GT have also proposed that the mid-Pleistocene transition from a 41-kyr glacial cycle to a 100-kyr cycle some 800 kyr ago may have been due to a general climate cooling that allowed extensive sea-ice cover to develop and resulted in the activation of the SIS mechanism at that time. However, no specific explanation of how the switch activation occurred was given. The SIS mechanism also results in a simple heuristic explanation for the timescale of the oscillation. Yet, the heuristic explanation in GT did not account explicitly for the fact that the glaciation stage takes significantly longer than the deglaciation stage. The asymmetry obtained in their model was thus a result of the (reasonable) choice of the model parameters, rather than of an explicit physical argument.

[3] The objective of this paper is to provide a detailed explanation for two features of the glacial oscillations: the transition from a dominant period of 41 kyr to one of 100 kyr in glacial cycles, and the asymmetry between the timescale of the glaciation and deglaciation. We show that both features arise naturally within the framework of the SIS glacial cycle mechanism (GT) as a possible result of the climate transition (or equivalently, bifurcation) which occurred about 800 kyr ago. In the mechanism proposed here, the transition occurs due to a cooling of the deep ocean which is known to have been warmer than the modern ocean prior to the mid-Pleistocene transition [*Billups et al.*, 1998; *McIntyre et al.*, 1999; *Ruddiman et al.*, 1989; *Marlow et al.*, 2000]. We do not specify the reason for the deep water cooling, but one may invoke reasons such as a change in the level of atmospheric $CO_2$ [*Raymo*, 1998; *Maasch and Saltzman*, 1990] or a gradual increase in ice volume [*Ghil and Childress*, 1987]. As a secondary objective of this paper, we introduce a highly simplified model of GT's SIS mechanism governed by few coupled ordinary differential equations. This simple model is used to demonstrate how both the 100-kyr timescale and the asymmetric glacial oscillation structure arise via the mid Pleistocene climate bifurcation, and is also useful in demonstrating the SIS mechanism in the simplest possible framework.

[4] There have been some alternative explanations for the asymmetry of the glaciation and deglaciation phases. *Le-Treut and Ghil* [1983] argued that the load-accumulation feedback between ice sheet mass balance and the bedrock isostatic rebound played a decisive role. *Pollard* [1983] and

[1]Now at Lamont-Doherty Earth Observatory of Columbia University, Palisades, New York, USA.


0883-8305/03/2001PA000627$12.00

*Watts and Hayder* [1984] have explained the rapid termination as the results of an ice sheet instabilities or enhanced calving. *Gallée et al.* [1992] found that a specified decrease in the albedo of aging snow during deglaciation induced rapid glacial termination in their model. Similarly, *Peltier and Marshall* [1995] attributed the rapid deglaciation to albedo variations due to dust loading together with marine-based ice sheet instability. It is fair to state, though, that a satisfactory detailed mechanism of the contrast between slow glaciation and rapid deglaciation is still missing.

[5] Before the 100-kyr glacial cycles of the past 800 kyr or so, glacial variability was dominated by a 41-kyr cycle which seemed very well correlated with Milankovitch forcing [*Ruddiman and Raymo*, 1988]. The transition to 100-kyr cycles may have been related to tectonic induced changes in $CO_2$ or to ice volume change as mentioned above [*Raymo*, 1998; *Maasch and Saltzman*, 1990; *Berger et al.*, 1999; *Saltzman and Sutera*, 1987; *Ghil and Childress*, 1987; *Paillard*, 1998], although alternative mechanisms were propose such as the interaction between ice sheets and the underlying bed [*Clark et al.*, 1999; *Clark and Pollard*, 1998], or other processes [*Mudelsee and Schulz*, 1997; *Deblonde and Peltier*, 1991]; see a recent review by *Elkibbi and Rial* [2001]. We propose here a new explicit mechanism for the transition. Moreover, one expects a mechanism for the asymmetry of the 100-kyr cycle to also account for the fact that the early Pleistocene 41-kyr cycles were symmetric. One clear advantage of the mechanism proposed in this paper is that it explains the symmetry of the 41-cycle, the asymmetry of the 100-kyr cycle, and the transition between the two in terms of the same mechanism.

[6] In the following section we deduce and describe a relation between the atmospheric temperature and the rates of accumulation and ablation of continental ice sheets. We then discuss the dependence of this relation between atmospheric temperature, accumulation and ablation on the temperature of the deep ocean. In section 3, we provide a heuristic explanation of the mid-Pleistocene climate transition in terms of the temperature–accumulation–ablation relations. We then proceed to describe the simplified SIS model equations used here in section 4. The model is used in section 5 to demonstrate how the asymmetry of the glacial cycle and transition from 41 to 100 kyr may have both arisen through the same mechanism of climate transition about 800 kyr ago. We conclude in section 6.

## 2. Accumulation–Ablation–Temperature Relations

[7] At the heart of the present paper lies the relation between the atmospheric temperature, sea-ice cover, and the rates of accumulation of snow over continental ice sheets and of their ablation. It is well known that warmer temperatures lead to a larger precipitation rate and thus to a larger rate of accumulation over continental ice sheets [*Miller and de Vernal*, 1992]. This effect was named the precipitation–temperature feedback [*Källén et al.*, 1979]. It results from the fact that very cold atmospheric temperatures lead to reduced atmospheric humidity and therefore to reduced precipitation. Similarly, when the temperature is cold enough for an extensive sea-ice cover to form, its albedo further cools the atmospheric temperature, and may divert snow storms away from continental ice sheets. The insulating effect of a sea-ice cover also limits the evaporation from the subpolar oceans, again leading to a reduction in the moisture available for precipitation over the land glaciers. The precipitation–temperature feedback has been documented in proxy records [e.g., *Lorius et al.*, 1985; *Jouzel et al.*, 1987; *Cuffey and Clow*, 1997; *Alley et al.*, 1993], model studies [*Charles et al.*, 1994], and was used in modeling the glacial cycle [*Källén et al.*, 1979; *Ghil et al.*, 1987; *Ghil*, 1994]. At yet higher temperatures, more and more of the precipitation falls as rain instead of snow and the actual accumulation over continental ice sheets then decreases with increasing temperature. Thus we expect the accumulation to increase with the temperature up to some limit, and then to decrease again. More specifically, the feedback between temperature and net ice sheet accumulation seems to depend on having higher winter temperatures, and to be further strengthened by lower summer temperatures [*Miller and de Vernal*, 1992].

[8] A novel point we make here is that this atmospheric temperature–accumulation relation varies as a function of the deep ocean temperature. We will show that this results in a different temperature–accumulation relation for the cold deep ocean of the late Pleistocene than for the warm deep ocean of the early Pleistocene.

[9] Consider first the case of a cold deep ocean. In this case there is a strong thermal gradient between the surface and deep ocean, and the resulting strong stratification significantly limits the vertical mixing between the surface and deep water. This effective decoupling between the deep and upper ocean has an important consequence regarding the behavior of sea-ice. As the atmospheric temperature decreases, the upper ocean is cooled fairly rapidly, not being too influenced by the deep ocean (which is also fairly cold anyway). At some critical atmospheric temperature, the near-surface ocean reaches the freezing temperature, and sea-ice begins to form at higher latitudes (vertical dashed lines in the lower panel of Figure 1). The ice-albedo feedback then results in further cooling of the atmosphere, which cools the ocean further and leads to the formation of more sea-ice. The sea-ice growth is self-limiting due to its insulating effects (GT), and eventually stops when the sea-ice cover is fairly extensive. Because the relevant heat capacity of the ocean in this scenario is only that of the upper ocean, the whole process takes only a few decades at most. Thus the sea-ice response is effectively immediate, as if it were a ''switch'' responding to a reduction of the atmospheric temperature. Once the sea-ice cover is large, its strong albedo effects on the atmospheric temperature and its insulating effect on the local evaporation from the subpolar oceans lead to a rapid decrease in the accumulation rate over the land glaciers (GT). The dependence of the accumulation on the atmospheric temperature in this scenario is depicted by the heavy solid line in the lower panel of Figure 1: the accumulation is low for cold atmospheric temperature when extensive sea-ice exists, jumps at a temperature $T_f$ when sea-ice melts, further increases with temperature for a while due to the temperature–precipitation feedback, and then decreases again for a warmer yet temperature.

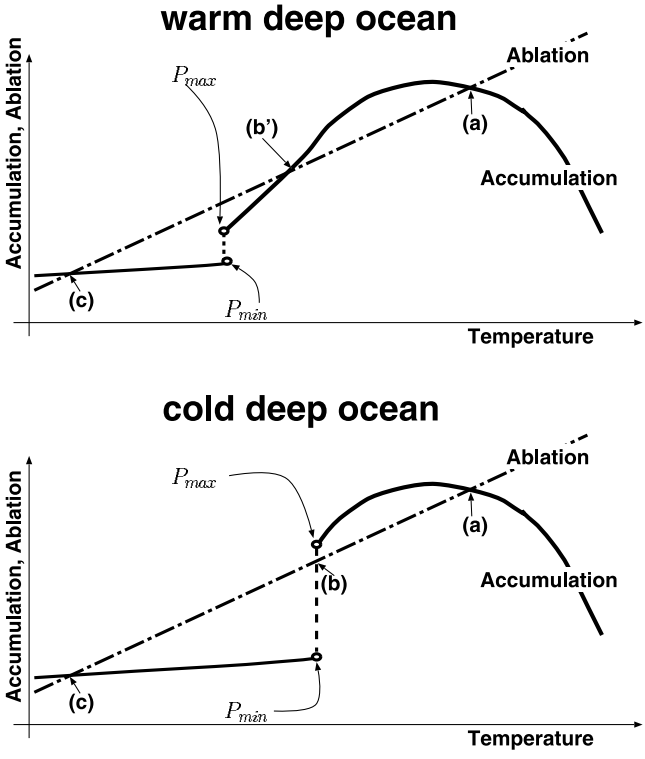


**Figure 1.** Schematic relations between accumulation (solid and dash) ablation (dash-dot) and temperature for different deep ocean temperatures. $P_{min}$ ($P_{max}$) are the rates of accumulation just after (before) the initiation of the sea-ice switch. Points (a) and (c) are unstable steady state points (see text) while points (b) and (b′) are stable. The glacial cycles are around the latter points.

[10] Next, let us consider the accumulation–temperature relation when the deep ocean is warm, as it seems to have been earlier than about 1 Ma [*Billups et al.*, 1998; *McIntyre et al.*, 1999; *Ruddiman et al.*, 1989; *Marlow et al.*, 2000]. In this case, the thermal difference between the upper and deep ocean is much reduced, and therefore their density difference is reduced, too. This leads to a significantly enhanced vertical mixing [*Gargett*, 1984] between the warm deep ocean and the surface water. The enhanced vertical mixing has two effects. First, it links the warm and deep ocean to the surface ocean very strongly, effectively making them a single system of a larger heat capacity. Second, the enhanced vertical mixing leads to a stronger thermohaline circulation (THC) [*Bryan*, 1987; *Lyle*, 1997] and therefore to a larger rate of deep water formation, which again creates a stronger link between the surface and deep ocean. A cooling of the atmospheric temperature cannot lead as easily to the formation of a sea-ice cover: the atmospheric cooling now needs to overcome both the stronger poleward heat transport by the enhanced THC, and the strong mixing of the surface water with the warm deep water. Thus, sea-ice does not form as rapidly as when the deep ocean is cold, even for the same atmospheric conditions. Sea-ice eventually forms, but at a colder atmospheric temperature than it does for a cold deep ocean. Once it forms, it has the same effect as explained above on the snow accumulation rate over ice sheets. The upper panel of Figure 1 shows the accumulation rate in this scenario, with the atmospheric temperature at which sea-ice forms again denoted by the vertical dashed line. This line is now shifted toward a colder atmospheric temperature relative to the cold deep ocean scenario of the figure's lower panel.

[11] As the deep ocean cooled over the past few millions of years, we expect the temperature–accumulation relation to have continuously changed from the configuration in the upper panel of Figure 1 to that in the lower panel. The implications of this change are discussed in the next section.

[12] Land-ice ablation is also expected to increase with increasing temperature due to enhanced melting, although as mentioned above, for a temperature range corresponding to the conditions during the late Pleistocene glacial cycles, we still expect net accumulation to increase with temperature more than ablation [*Miller and de Vernal*, 1992]. The ice sheets ablation rate is assumed here to be a weakly increasing linear function of the temperature, and is shown as heavy dash-dot lines in Figure 1. We assume that this function does not depend on the deep-ocean temperature and so this line is the same in both panels. Another point, taken into consideration below, is that ablation is also strongly controlled by summer solar radiation: the small heat capacity of the ice sheets' surface makes its temperature a strong function of the radiation. Therefore the radiation during the summer melting season dictates the melt/ablation rate [*Held*, 1982]. Note that the feedback between temperature and net ice sheet accumulation (including precipitation as well as melting) has been questioned in some recent studies, although mostly in the context of greenhouse warming, due to the role of melt processes at higher temperatures [e.g., *Bromwich et al.*, 1999; *Ohmura et al.*, 1996; *Thompson and Pollard*, 1997].

## 3. Mid-Pleistocene Climate Transition Scenario

[13] The consequences of Figure 1 contain the main message of this paper, and we wish to explain them even before getting to the technicalities of the actual model description. Note that the ablation curve crosses either accumulation curve at three points. These points represent atmospheric temperatures at which the ablation rate of the continental ice sheets equals the accumulation rate, and one may therefore expect a steady state for the land-ice volume at these points. However, it is simple to see that only one of these three points represents a stable steady state. Consider, for example, point (a) where the accumulation curve crosses the ablation curve, at the warmest of the three temperatures in question. Assume that the climate system is at this point, and consider a small cooling perturbation to the temperature. As a result of this cooling, the ablation decreases, while the accumulation either increases (as shown in the figure) or decreases at a lower rate than the ablation. To the left of point (a), the ablation is therefore smaller than the accumulation, leading to a growth of the ice sheets. The resulting increase in land-ice albedo leads to further cooling, and thus to a positive feedback which leads the climate system further away to the left of point (a). A similar analysis follows for a warming perturbation to point (a) which will lead to the

climate state moving further to the right of this point. This is, therefore, an unstable steady state. Point (c) at the lowest of the three fixed-point temperatures, is similarly unstable, while point (b′) in the upper panel of Figure 1 is stable: a small cooling perturbation away from point (b′), for example, leads to the ablation being larger than the accumulation, which decreases the land-ice volume and area. This leads to a smaller land-ice albedo, and therefore to a warming that reduces the initial perturbation and cancels it, leading back to the steady state at point (b′).

[14] The global stability behavior for the warm deep ocean scenario is thus as follows. Any initial state to the right of point (a) will lead to a decrease in land-ice volume, to a climate warming, and to further ice sheet melting. Additional feedbacks not considered here may, of course, stop the system from getting into a runaway warming scenario. An initial state to the left of point (c) will similarly lead to a climate cooling, and further (possibly unstable) expansion of land-ice. Any state between points (a) and (c) will result in a climate evolution toward the stable steady state at (b′), where the ablation balances the accumulation rate. Climate stability is normally looked at from the point of view of temperature and albedo [*North et al.*, 1981; *Ghil and Childress*, 1987], but not of accumulation and precipitation. It is interesting to note that the accumulation-ablation perspective of Figure 1 indicates that the crossing of the accumulation and ablation curves at point (c) is necessary. Without it, all the states to the left of point (b′) will lead the climate system back to the steady state of point (b′) and there would be no possibility of an unstable ice sheet growth. The latter is thus only possible due to the existence of the unstable point (c). Similarly, the crossing at point (a) is necessary or else no unstable warming feedback is possible. We conclude that the general qualitative structure of the accumulation-ablation-temperature plots of Figure 1, with their 3 intersections, is necessarily robust and likely to be quite realistic.

[15] Allowing now for the fact that the ablation actually also depends on the summer solar radiation, we note that orbital variations in summer insolation at middle and high latitudes should lead to small oscillations of the land-ice volume around point (b′). These oscillations in the land-ice volume should be symmetric and follow the Milankovitch–Berger summer insolation rather closely [*Milankovitch*, 1930; *Berger*, 1978]. This scenario agrees with the symmetry of the observed record prior to about 800 kyr ago [*Ruddiman and Raymo*, 1988].

[16] Things are slightly more complex for the cold deep ocean scenario. Points (a) and (c) again represent unstable steady states due to the interception of the accumulation and ablation curves. The two curves also cross for this scenario at point (b), where the accumulation curve is vertical (dashed). As explained above, the switch-like behavior of the sea-ice in this scenario does not allow the accumulation to actually remain constant at point (b). Instead, it can only jump between the two states marked by the open circles above and below (b). As shown by GT, the climate behavior around point (b) is characterized by glacial-interglacial oscillations with a saw-tooth structure and a 100-kyr timescale, as observed over the past 700–800 kyr.

[17] We thus conclude that a shift from a warm deep ocean to a cold deep ocean also results in a shift from a symmetric, purely forced oscillation in land-ice volume with the Milankovitch-Berger periodicities of 20 and 41 kyr to an asymmetric, self-sustained oscillation with a 100-kyr timescale and a saw-tooth structure. In the next section we illustrate this scenario using a simple mathematical model.

## 4. Model

[18] The SIS mechanism was proposed in GT using a fairly detailed box model of the ocean, atmosphere, land-ice and sea-ice. For the purpose of the present paper, and also in order to make the SIS mechanism easier to understand, we present a simplified model and use it for investigating the mid-Pleistocene climate transition. Another motivation for using a simpler model than that of GT is that while the deep ocean cooling on which the mechanism proposed here is based was indeed seen in proxy climate indicators, the exact cause and rate of cooling is yet unknown. Thus our only possible way to proceed is to specify the cooling rather than model it explicitly, and the model used here is specifically formulated to allow for such a specification. One could possibly specify the deep ocean cooling in the more detailed GT box model, but wishing to use the simplest possible model for a given task, we proceed with the following simpler model.

[19] The model used here has two prognostic variables for which explicit time evolution equations are provided: the land-ice volume $V_{land\text{-}ice}$ and a temperature $T$ that crudely represents the atmospheric temperature, yet is influenced by the larger heat capacity of the upper ocean. There are also several diagnostic variables of physical quantities that adjust very quickly to the prognostic model variables, and thus may simply be parameterized in terms of the prognostic variables. These include the sea-ice area $a_{sea\text{-}ice}$ and the precipitation over the continental ice sheets $P$ which is the source of their growth. The ice-albedo feedback leads to a very rapid growth of the sea-ice until it covers a significant area of the high-latitude ocean, where it is then self-limiting and its growth is stopped (GT). The sea-ice area is therefore assumed in the present model to simply be at one of two states, depending on the temperature $T$ and on the critical atmospheric temperature $T_f$ at which the near-surface ocean reaches the freezing temperature and sea-ice forms; as explained above, the value of $T_f$ depends in turn on the deep-water temperature. In the present simple model $T_f$ is prescribed to have a higher value for the case of the cold deep ocean and a lower one when the deep ocean is warm. We thus have:

$$a_{sea-ice} = \begin{cases} I_s^0 & T < T_f \\ 0 & T > T_f \end{cases}. \qquad (1)$$

The precipitation/accumulation (P) over the ice sheets depends on two factors. First, the temperature of the system dictates the moisture content of the atmosphere, via the Clausius–Clapeyron relation [*Peixoto and Oort*, 1991],

$$q(T) = q_r\ \epsilon_q\ A\ \exp(-B/T)/p_s,$$

where $q_r$ is some assumed relative humidity, $p_s$ is the surface pressure, and ($\epsilon_q$, $A$, $B$) are constants. As a result, a warm temperature leads to more atmospheric moisture being available and to more precipitation over the ice sheets. The second factor affecting precipitation is that an extensive sea-ice cover during cold time intervals limits local evaporation from the subpolar oceans, and redirects storms away from the ice sheets, thus limiting again the amount of precipitation over them. The combined parameterization for the precipitation–accumulation is, therefore,

$$P(T, a_{sea-ice}) = [P_0 + P_1 q(T)] \times \left(1 - \frac{a_{sea-ice}}{a_{ocn}}\right),$$

where the first parenthesis represents the precipitation–temperature feedback through the dependence of the humidity $q(T)$ on the temperature, and the second represents the effect of the sea-ice. Additionally, when the temperature increases beyond a critical temperature $T_{rain}$, the precipitation could be assumed to be in the form of rain, so that accumulation is reduced by some factor like $\exp[(T - T_{rain})/\Delta T_{rain}]$. Since we study glacial oscillations only in the neighborhood of point (b) in Figure 1, it is not necessary to actually add this factor to our model formulation and we do not do so here.

[20] Finally, based on the discussion in section 2, and in order to simulate the slow cooling of the deep ocean over the past 2 Ma and the mid-Pleistocene transition, we make the atmospheric temperature at which sea-ice forms, $T_f$ a slowly varying function of time, varying linearly in time from $T_f^{init}$ to $T_f^{final}$. Figure 2 shows the ablation and precipitation as a function of the model temperature $T$, for both the initial time of the model run and the final time.

[21] The model equation for the land-ice is a simple mass balance accounting for both precipitation and ablation that follows [*Weertman*, 1976; *Källén et al.*, 1979]:

$$\frac{dV_{land-ice}}{dt} = P(T, a_{sea-ice}) - S_{abl}(T, t).$$

The ablation is assumed to be a weak function of the temperature and to also depend on Milankovitch summer radiation (see section 2 and references there):

$$S_{abl}(T, t) = S_0 + S_M M(t) + S_T(T - 273.), \qquad (2)$$

where $M(t)$ is the deviation of the summer insolation at 65N [*Berger*, 1978] from its long-term mean value, and normalized by its standard deviation. The temperature equation includes the effects of incoming solar radiation, outgoing long wave radiation, and the albedo of both land and sea-ice (neglecting the smaller albedo of open ocean and ice free land areas) [*Källén et al.*, 1979; *Le-Treut and Ghil*, 1983]:

$$\frac{C_{ocn}}{a_{ocn}}\frac{dT}{dt} = -\varepsilon\sigma T^4 + H_s\left(1 - \alpha_s \frac{a_{sea-ice}}{a} \quad -\alpha_L \frac{a_{land-ice}}{a}\right) .(1 - \alpha_C),$$

where $C_{ocn}$ reflects the heat capacity of the atmosphere and upper ocean, and $a$ is the total area, of land plus ocean. (See Table 1 for explanation of other symbols.) The relation between land-ice volume and area is based on a parabolic glacier shape [*Weertman*, 1976; *Ghil*, 1994] and is given by

$$a_{land-ice} = \left(L^{E-W}\right)^{1/3}\left(V_{land-ice}/\left(2\lambda^{1/2}\right)\right)^{2/3}.$$

[22] The model parameters used in the above equations are summarized in Table 1. The model is integrated in time using an Adams time stepping scheme (NAG routine D02CJF).

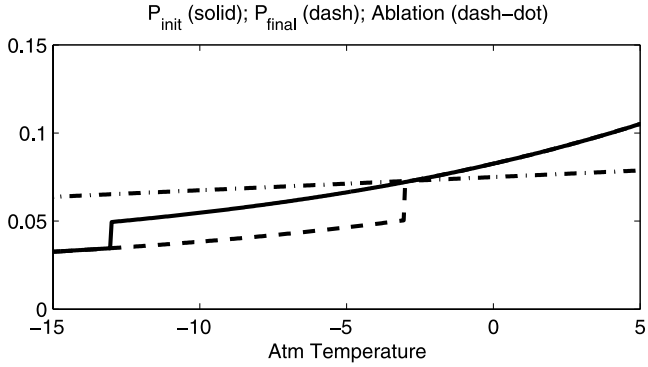


**Figure 2.** Time–mean ablation (dash–dot, obtained by setting $S_M = 0$ in 2), and precipitation/accumulation (in Sv) as function of temperature for initial (solid) and final (dash) times, as used in the model run described in the text. To simulate the deep ocean cooling, $T_f$ in (1) was made to vary linearly from $-13$°C 1.5 Ma BP to $-3$°C at 500 kyr BP and was then kept constant.

## 5. Model's Mid-Pleistocene Climate Transition

[23] Figure 3 shows the model results for a slowly varying deep-ocean temperature. The results exhibit a transition at about 800 kyr ago. Previous to the climate transition, the accumulation and ablation curves cross at a stable steady state point similar to point (b′) in the upper panel of Figure 1. The existence of Milankovitch forcing, with its linear effect on summer melting, forces the system into a simple linear symmetric oscillation around the steady state. Beyond the transition, the accumulation and ablation curves cross at a point like (b) in the lower panel of Figure 1, where the SIS is activated and the 100-kyr oscillations therefore occur. Because of the presence of the Milankovitch forcing, the sea-ice switch is activated even slightly before the ablation crosses the accumulation curve along the dashed line in Figures 1 and 2. It is enough for the ablation to get sufficiently close to the transition point, and the Milankovitch-induced land-ice and temperature variations are then sufficient to bring the system to a cold enough temperature at which sea-ice forms and the sea-ice switch oscillations begin.

[24] We refer the readers to GT for an explanation of the SIS glacial cycle mechanism. In order to explain how the asymmetric structure of the oscillation arises from the mid-Pleistocene transition, however, we need to briefly repeat

**Table 1.** Model Parameters

| Symbol | Value, units | Explanation |
|---|---|---|
| $q_l$, $\epsilon_q$, $A$, $B$, $P_s$ | 0.7, 0.622, 2.53 $10^{11} Pa$, 5.42 $10^3 K$, $10^5 Pa$ | Clausius–Clapeyron parameters |
| $P_0$, $P_1$ | 0.06 $Sv$, 40 $Sv/Pa$ | accumulation parameterization |
| ($S_0$, $S_M$, $S_T$) | 0.15 $Sv$, 0.08 $Sv$, 0.0015 $Sv/K$ | ablation parameterization |
| $\varepsilon$ | 0.64 | emissivity |
| $\sigma$ | 5.67 $10^{-8}$ $Wm^{-2}$ $K^{-4}$ | Boltzman's constant |
| $H_s$ | 350.0 $Wm^{-2}$ | incoming solar radiation |
| ($\alpha_s$, $\alpha_L$, $\alpha_C$) | (0.65, 0.7, 0.27) | albedo of sea ice, land ice and clouds |
| $C_{ocn}$ | $C_P V_{ocn} \rho_0$, $JK^{-1}$ | atmosphere & upper ocean's heat capacity |
| ($a_{ocn}$, $a_{land}$) | (20 $10^6$ $km^2$, 20 $10^6$ $km^2$) | area of land and ocean. |
| $V_{ocn}$ | 21.6 $10^6$ $km^3$ | volume of upper ocean. |
| $I_s^0$ | 0.3 $a_{ocn}$ | max ice cover during switch-on periods |
| $\lambda$ | 10 m | glacier model |
| $L^{E-W}$ | 4000 km | (fixed) width of land and glacier |

the heuristic argument for the timescale of the glacial cycle in the SIS mechanism. Let the variable part of the land glaciers have a volume $\Delta V$. Assume also that the ice sheet is fed at either a maximum accumulation (source) rate $P_{\max}$ (during the buildup stage) or at a minimum rate $P_{\min}$ (during deglaciation), and further assume a constant ablation (sink) rate $S$. The total timescale of a complete cycle is then

$$\tau = \tau_{\text{buildup}} + \tau_{\text{deglaciation}} = \frac{\Delta V}{P_{\max} - S} + \frac{\Delta V}{S - P_{\min}}. \quad (3)$$

[25] For reasonable choices of the different parameters, one obtains $\tau \approx 100$ kyr (GT), and the minimum of $\tau$ as function of the sink amplitude is $\sim$50 kyr and occurs for a symmetric oscillation ($\tau_{\text{buildup}} = \tau_{\text{deglaciation}}$), when $S = (P_{\max} + P_{\min})/2$. If the ablation increases, the total period gets longer, the glaciation (buildup) time gets longer and the deglaciation time shorter, so that as we approach the bifurcation point, the cycle becomes more asymmetric. Figure 1 shows that as the deep ocean cools enough for the SIS to be activated, the ablation crosses the accumulation curve at the vertical dashed line in that figure, which represents the accumulation jump due to the sea-ice switch. The ablation–accumulation crossing location right after the climate transition is necessarily such that the ablation is close to $P_{\max}$. This immediately implies, according to (3), that the glaciation time should be longer than the deglaciation time, as observed. This is an important point and one of our main results: as the slow deep ocean cooling leads to

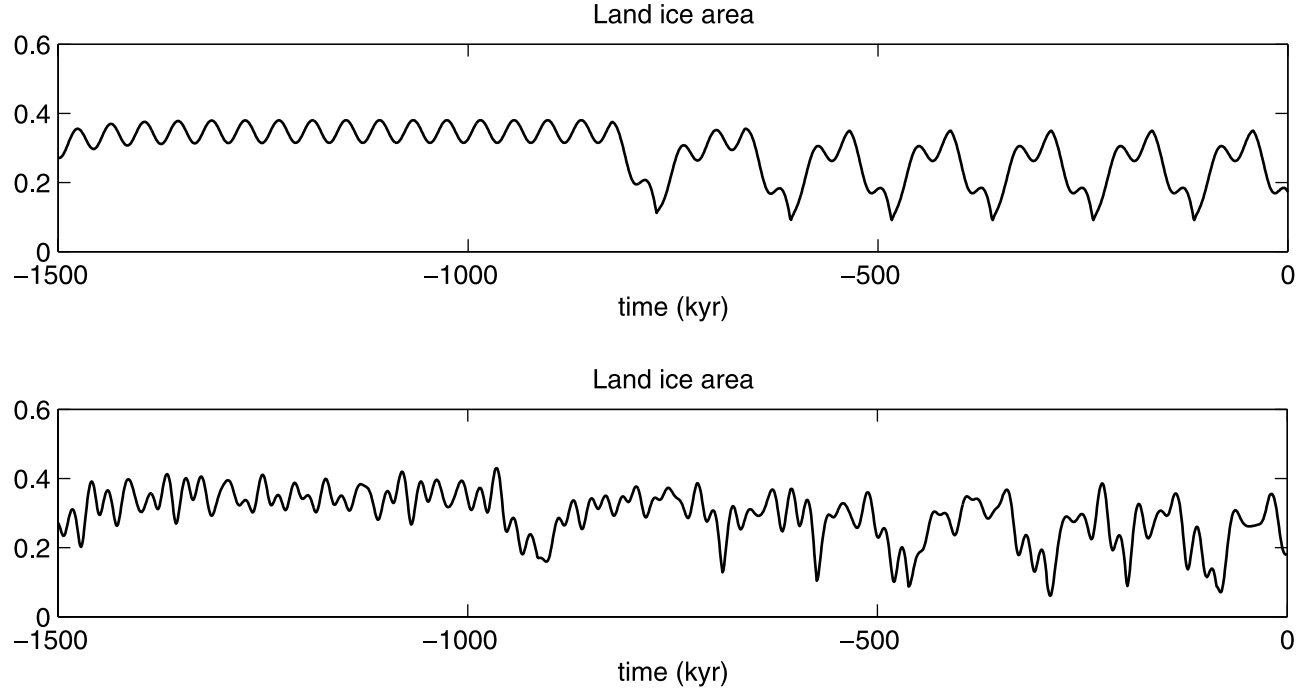


**Figure 3.** Model results for slowly varying deep ocean temperature. Shown is a time series of the fraction of land area covered by land ice. The transition from obliquity and precession (20 and 41 kyr) dominated cycles to 100 kyr ones is seen around −800 kyr. Upper panel: using an idealized insolation curve with a simple periodicity of 41 kyr. Lower panel: using actual Milankovitch summer radiation at 60N.

the qualitative transition from the small-amplitude, purely linear oscillations forced by obliquity and precession, to 100-kyr oscillations triggered by the SIS, the latter are necessarily highly asymmetric right after the transition! The fact that the 100-kyr oscillations are asymmetric over the past 700–800 kyr indicates, according to this scenario, that the climate system is not far from the hypothetical bifurcation point which gives rise to the initiation of the 100-kyr oscillations.

[26] Note that we expect a shortening of the glacial cycle timescale past the transition point (between the mid-Pleistocene like transition which is at about 800 kyr in this plot and 0 kyr). This shortening of timescale is expected from equation (3), due to the increasing distance between the ablation and point $P_{\max}$ in the lower panel of Figure 1, as the deep ocean cools and point $P_{\max}$ moves to the right in that schematic figure. Actually, we do not know if the deep ocean continued to cool beyond the mid-Pleistocene transition, nor do we know the real cooling rate of the deep ocean. It is thus unclear how far away we are from the transition point (in term of the deep ocean temperature) and which period and structure of the glacial-interglacial we should expect. (The years on the time axes should not be taken at face value!).

[27] There are a couple of issues that are worth noting at this stage: First, observations indicate that most of the deep ocean cooling has occurred long before the mid-Pleistocene transition, and only a slow cooling continued to the time of the transition itself. This does not contradict our mechanism. We only require that the system crosses the threshold in which the ablation curve crosses the accumulation curve at a point like (b) instead of (b′) in Figure 1, and the rate of the cooling leading to this threshold crossing does not matter. Second, note that our pretransition model time series (lower panel of Figure 3) is dominated by precession (20 kyr) which is the main contribution to the variability of summer radiation at 65N, while the observations are more of an obliquity-dominated record [*Raymo et al.*, 1990]. There are indeed some recent suggestions that the relevant Milankovitch forcing to use is indeed the gradient of the solar radiation between high and low latitudes, which is dominated by obliquity (M. E. Raymo and K. Nisancioglu, Milankovitch's other unsolved mystery—The 41 kyr world, preprint, 2002). Given that the dynamical balances behind this suggestion are still unresolved, we refrain from additional discussion of this issue.

[28] There is one notable difference between the model results of Figure 3 and the observed $\delta^{18}O$ record [*Raymo et al.*, 1990]. Taking the $\delta^{18}O$ at face value as a proxy for ice volume, it seems to show that the symmetric oscillations prior to the Mid-Pleistocene transition and the 100-kyr oscillations after the transition have been around the same mean, with the former oscillations merely having a smaller amplitude. In our model results, the amplitude of the obliquity and precession dominated linear oscillation prior to the transition is indeed smaller, as in the observed record, yet it is around a higher mean value (Figure 3). It is possible that some of this difference is due to the fact that $\delta^{18}O$ incorporates additional effects beyond the land-ice volume such as the temperature and salinity of the ocean [*Shackleton*, 2000]. It is also possible, of course, that some missing physics in our highly idealized model accounts for this difference.

## 6. Conclusions

[29] We have proposed here a specific detailed mechanism for the mid-Pleistocene climate transition from shorter period, small amplitude, symmetric glacial cycles, to 100-kyr asymmetric oscillations. According to this mechanism, the former oscillations are small-amplitude, purely forced oscillations about a steady state of the continental ice sheets that are driven by Milankovitch radiation changes. At the time of the transition, a cooling of the deep ocean allowed an extensive sea-ice cover to develop, and enabled the sea-ice switch glacial cycle mechanism of [*Gildor and Tziperman*, 2000], resulting in asymmetric, saw-tooth shaped 100-kyr oscillations.

[30] The asymmetry of the oscillation, with gradual glaciations and rapid deglaciations, is related in this mechanism to the fact that the mean value of the ice sheet ablation is not far from the maximum rate of snow accumulation during warm periods. We have shown that this proximity of ablation and accumulation is to be expected if the 100-kyr glacial cycles have indeed started due to a climate transition driven by a gradual cooling of the deep ocean. We also explained that had the general climate cooling continued, the timescale of the glaciation phase would be shortened, and that of the deglaciation would be lengthened, leading to a more symmetric glacial cycle. In today's climate, ablation and accumulation rates are very close, making it impossible to confidently determine the mass balance of the Greenland-ice sheet [see, e.g., *Paterson*, 1994; *Davis et al.*, 1998]. This observed proximity of ablation and accumulation strengthens the case for the glacial cycles being near the transition (bifurcation) point leading from 41 kyr to 100 kyr oscillations.

[31] Unlike some previous explanations of the asymmetry of the 100 kyr glacial cycles, our mechanism also explains why the glacial oscillations prior to 800 kyr ago were symmetric. We were therefore able to provide a single unified mechanism for the changes in the nature of the oscillation (i.e. changes in period and symmetry), for the 100-kyr glacial timescale of the late Pleistocene, and for the transition between the two kinds of glacial oscillations.

[32] The model used here is highly idealized and some of our arguments are admittedly speculative. However, the explanation of the mid-Pleistocene glacial cycle transition and of the glacial cycle asymmetry which are provided here supplement the predictions based on the sea-ice switch mechanism for the general structure of the land-ice record [*Gildor and Tziperman*, 2001b], for the role of Milankovitch forcing and the climate transition of 800 kyr ago [*Gildor and Tziperman*, 2000], for a teleconnection mechanism between the hemispheres, and for the physical processes behind glacial-interglacial $CO_2$ variations [*Gildor and Tziperman*, 2001a]. We therefore feel that the explanation of the mid-Pleistocene transition which is provided here further strengthens the case for the SIS mechanism. It

would be most interesting to test some of the specific falsifiable predictions of this mechanism, which involve the absence of northern extensive sea-ice cover till the mid-Pleistocene, the relative phase between sea-ice cover and land-ice deglaciations, and the relative phase between atmospheric $CO_2$ and global ice volume, using for example new proxies of sea-ice that may become available in the near future based on recently developed proxies [e.g., *de Vernal and Hillaire-Marcel*, 2000; *Sarnthein et al.*, 1995].

[33] **Acknowledgments.** We thank Yossi Ashkenazy, Mark Cane, Michael Ghil and two anonymous reviewers for their most useful and constructive comments. This work is partially supported by the Israeli–US Binational Science Foundation.

## References


Alley, R. B., et al., Abrupt increase in Greenland snow accumulation at the end of the Younger Dryas event, *Nature*, *362*, 527–529, 1993.

Berger, A., Long-term variations of daily insolation and Quaternary climate changes, *J. Atmos. Sci.*, *35*, 2362–2367, 1978.

Berger, A., X. Li, and M. Loutre, Modelling northern hemisphere ice volume over the last 3 Ma, *Quat. Sci. Rev.*, *18*, 1–11, 1999.

Billups, K., A. C. Ravelo, and J. C. Zachos, Early Pliocene deep water circulation in the western equatorial Atlantic: Implications for high-latitude climate change, *Paleoceanography*, *13*, 84–95, 1998.

Bromwich, D. H., Q. S. Chen, Y. F. Li, and R. I. Cullather, Precipitation over Greenland and its relation to the North Atlantic Oscillation, *J. Geophys. Res.*, *104*, 22,103–22,115, 1999.

Bryan, F., Parameter sensitivity of primitive equation ocean general circulation models, *J. Phys. Oceanogr.*, *17*, 970–985, 1987.

Charles, C. D., D. Rind, J. Jouzel, R. D. Koster, and R. G. Fairbanks, Glacial-interglacial changes in moisture sources for Greenland: Influences on the ice core record of climate, *Science*, *263*, 508–511, 1994.

Clark, P., R. Alley, and D. Pollard, Northern hemisphere ice-sheet influences on global climate change, *Science*, *286*, 1104–1111, 1999.

Clark, P. U., and D. Pollard, Origin of the middle Pleistocene transition by ice sheet erosion of regolith, *Paleoceanography*, *13*, 1–9, 1998.

Cuffey, K., and G. Clow, Temperature, accumulation, and ice sheet elevation in central Greenland through the last deglacial transition, *J. Geophys. Res.*, *102*, 26,383–26,396, 1997.

Davis, C. H., C. A. Kluever, and B. J. Haines, Elevation change of the southern Greenland ice sheet, *Science*, *279*, 2086–2088, 1998.

Deblonde, G., and W. R. Peltier, A one-dimensional model of continental ice volume fluctuations through the Pleistocene: Implications for the origin of the mid Pleistocene climate transition, *J. Clim.*, *4*, 318–344, 1991.

de Vernal, A., and C. Hillaire-Marcel, Sea-ice cover, sea-surface salinity and halo-/thermocline structure of the northwest North Atlantic: Modern versus full glacial condition, *Quat. Res.*, *9*, 65–85, 2000.

Elkibbi, M., and J. Rial, As outsider's review of the astronomical theory of climate: Is the eccentricity-driven insolation the main driver of the ice ages?, *Earth Sci. Rev.*, *56*, 161–177, 2001.

Gallée, H., J. VanYpersele, T. Fichefet, I. Marsiat, C. Tricot, and A. Berger, Simulation of the last glacial cycle by a coupled, sectorially averaged climate-ice sheet model, 2, Response to insolation and $CO_2$ variations, *J. Geophys. Res.*, *97*, 15,713–15,714, 1992.

Gargett, A., Vertical eddy diffusivity in the ocean interior, *J. Mar. Res.*, *42*, 359–393, 1984.

Ghil, M., Cryothermodynamics: The chaotic dynamics of paleoclimate, *Physica D*, *77*, 130–159, 1994.

Ghil, M., and S. Childress, *Topics in Geophysical Fluid Dynamics: Atmospheric Dynamics*, *Dynamo Theory and Climate Dynamics*, Springer-Verlag, New York, 1987.

Ghil, M., A. Mullhaupt, and P. Pestiaux, Deep water formation and Quaternary glaciations, *Clim. Dyn.*, *2*, 1–10, 1987.

Gildor, H., and E. Tziperman, Sea ice as the glacial cycles climate switch: Role of seasonal and orbital forcing, *Paleoceanography*, *15*, 605–615, 2000.

Gildor, H., and E. Tziperman, Physical mechanisms behind biogeochemical glacial-interglacial $CO_2$ variations, *Geophys. Res. Lett.*, *28*, 2421–2424, 2001a.

Gildor, H., and E. Tziperman, A sea-ice climate-switch mechanism for the 100 kyr glacial cycles, *J. Geophys. Res.*, *106*, 9117–9133, 2001b.

Held, I., Climate models and the astoromical theory of ice age, *Icarus*, *50*, 449–461, 1982.

Jouzel, J., C. Lorius, J. R. Petit, C. Genthon, N. I. Barkov, V. M. Kotlyakov, and V. M. Petrov, Vostok ice core: A continuous isotope temperature record over the last climatic cycle (160,000 years), *Nature*, *329*, 403–407, 1987.

Källén, E., C. Crafoord, and M. Ghil, Free oscillations in a climate model with ice-sheet dynamics, *J. Atmos. Sci.*, *36*, 2292–2303, 1979.

Le-Treut, H., and M. Ghil, Orbital forcing, climatic interactions, and glaciations cycles, *J. Geophys. Res.*, *88*, 5167–5190, 1983.

Lorius, C., J. Jouzel, C. Ritz, L. Merlivat, N. Barkov, Y. Korotkevich, and V. Kotlyakov, A 150,000-year climatic record from Antarctic ice, *Nature*, *316*, 591–596, 1985.

Lyle, M., Could early Cenozoic thermohaline circulation have warmed the poles?, *Paleoceanography*, *12*, 161–167, 1997.

Maasch, K., and B. Saltzman, A low-order dynamical model of global climatic variability over the full Pleistocene, *J. Geophys. Res.*, *95*, 1955–1963, 1990.

Marlow, J. R., C. Lange, G. Wefer, and A. Rosell-Mele, Upwelling intensification as part of the Pliocene–Pleistocence climate transition, *Science*, *290*, 2288–2291, 2000.

McIntyre, K., A. C. Ravelo, and M. L. Delaney, North Atlantic intermediate waters in the late Pliocene to early Pleistocene, *Paleoceanography*, *14*, 324–335, 1999.

Milankovitch, M., Mathematische Klimalehre und Astronomische Theorie der Klimaschwankungen I, in *Handbuch der Klimatologie*, edited by I. W. Koppen and R. Geiger, Verlag Borntrager, 1930.

Miller, G., and A. de Vernal, Will greenhouse warming lead to Northern Hemisphere ice-sheet growth?, *Nature*, *355*, 244–246, 1992.

Mudelsee, M., and M. Schulz, The Mid-Pleistocene climate transition: Onset of 100 ka cycle lags ice volume build-up by 280 ka, *Earth Planet. Sci. Lett.*, *151*, 117–123, 1997.

North, G., R. Cahalan, and R. Moeng, Energy balance climate models, *Rev. Geophys. Space Phys.*, *19*, 90–121, 1981.

Ohmura, A., M. Wild, and L. Bengtsson, A possible change in mass balance of Greenland and Antarctic ice sheets in the coming century, *J. Clim.*, *9*, 2124–2135, 1996.

Paillard, D., The timing of Pleistocene glaciations from a simple multiple-state climate model, *Nature*, *391*, 378–381, 1998.

Paterson, W., *The Physics of Glaciers*, 3rd ed., Pergamon, New York, 1994.

Peixoto, J., and A. Oort, *Physics of Climate*, Am. Inst. of Phys., New York, 1991.

Peltier, W., and S. Marshall, Coupled energy-balance/ice-sheet model simulations of the glacial cycles: A possible connection between terminations and terrigenous dust, *J. Geophys. Res.*, *100*, 14,269–14,289, 1995.

Pollard, D., A coupled climate-ice sheet model applied to the Quaternary ice ages, *J. Geophys. Res.*, *88*, 7705–7718, 1983.

Raymo, M., Glacial puzzles, *Science*, *281*, 1467–1468, 1998.

Raymo, M. E., W. F. Ruddiman, N. J. Shackleton, and D. W. Oppo, Evolution of Atlantic-Pacific $\delta^{13}C$ gradients over the last 2.5 my, *Earth Planet. Sci. Lett.*, *97*, 353–368, 1990.

Ruddiman, W., and M. Raymo, Northern Hemisphere climate regimes during the past 3 Ma: Possible tectonic connections, *Philos. Trans. R. Soc. London, Ser. B*, *318*, 411–430, 1988.

Ruddiman, W., M. Raymo, D. Martinson, B. Clement, and J. Backman, Pleistocene evolution: Northern hemisphere ice sheets and North Atlantic ocean, *Paleoceanography*, *4*, 353–412, 1989.

Saltzman, B., and A. Sutera, The mid-Quaternary climate transition as the free response of a three varable dynamical models, *J. Atmos. Sci.*, *44*, 236–241, 1987.

Sarnthein, M., et al., Variations in the surface ocean paleoceanography in the Atlantic between 50N and 80N: A time slice record, *Paleoceanography*, *10*, 1063–1094, 1995.

Shackleton, N., The 100,000-year ice-age cycle identified and found to lag temperature, carbon dioxide, and orbital eccentricity, *Science*, *289*, 1897–1902, 2000.

Thompson, S. L., and D. Pollard, Greenland and Antarctic mass balances for present and doubled atmospheric CO2 from the GENESIS version-2 global climate model, *J. Clim.*, *10*, 871–900, 1997.

Watts, R., and E. Hayder, A two-dimensional, seasonal, energy balance climate model with continents and ice sheets: Testing the Milankovitch theory, *Tellus*, *36*, 120–131, 1984.

Weertman, J., Milankovitch solar radiation variations and ice age ice sheet sizes, *Nature*, *261*, 17–20, 1976.


H. Gildor, Lamont-Doherty Earth Observatory, Columbia University, Palisades, NY, USA.

E. Tziperman, Environmental Sciences, Weizmann Institute of Science, Rehovot 76100, Israel. (eli@beach.weizmann.ac.il)